SQUIDs, brains and gravity waves

Superconducting quantum interference devices are so sensitive to magnetic flux that they can map the tiny magnetic fields emanating from the human brain and detect the submicroscopic motions of gravity-wave detectors.

John Clarke

▶ A lonely instrument in Baja California records tiny fluctuations in the Earth's magnetic field, giving valuable information on the location of geothermal energy.[1]

▶ An extremely quiet amplifier detects electrical noise generated by the fluctuating spins in a collection of chlorine nuclei—the first observation of nuclear-spin noise.[2]

▶ Superconducting gradiometers in liquid helium measure tiny fluctuating magnetic fields emanating from the human brain (see figure 1), pinpointing the source of the electrical discharge associated with focal epilepsy.[3]

▶ An aluminum bar weighing 4800 kg and cooled to 4.2 K rests in a vacuum chamber at Stanford University, working as the world's most sensitive monitor of gravitational radiation.[4]

These remarkably different measurements have one thing in common: They are all made by means of superconducting quantum interference devices. The SQUID, which is built from either one or two Josephson junctions and which operates at a temperature of a few kelvins, is a magnetic-flux detector of unsurpassed sensitivity. By connecting it to a suitable circuit one may make sensitive measurements of a wide range of physical parameters, including voltage, resistance, magnetic field gradient, magnetic susceptibility and displacement. Indeed, the sensitivity of the SQUID in measuring these quantities makes possible many experiments that otherwise could not even be contemplated.

The first type of SQUID—the two-junction or dc SQUID—appeared in 1964 and was quite widely used by low-temperature physicists. The year 1970 saw the appearance[5] of the single-junction or rf SQUID, which became commercially available and therefore much more widely used than the dc device, particularly by non-specialists working outside the confines of the low-temperature laboratory. However, in the mid-1970s the realization that the dc SQUID was potentially much more sensitive than the rf SQUID, together with the coming of age of thin-film technology that made it no more difficult to make two junctions than to make one, led to extensive development of the dc SQUID. Thus, in the first part of this article I concentrate on the dc SQUID, looking at how it works, how the development of a theory for its noise led to much higher sensitivities and how typical devices are fabricated. After a brief description of the rf SQUID, I will discuss how either type can be used for a variety of measurements. Finally, I look at two particular applications—neuromagnetism and gravity-wave antennas—that take advantage of the extreme sensitivity of SQUIDs in very different ways.

John Clarke is professor of physics at the University of California, Berkeley, and a faculty senior scientist at Lawrence Berkeley Laboratory.

Superconductivity

The microscopic theory of superconductivity[6] developed by John Bardeen, Leon Cooper and Robert Schrieffer tells us that below the superconducting transition temperature, which is typically a few kelvins, at least some of the free electrons in a superconducting material are bound together in pairs. Each of these "Cooper pairs" consists of two electrons with opposite spins and, in the absence of applied currents or magnetic fields, equal and opposite momenta, so that the net spin and net momentum are both zero. The pairs condense into a single *macroscopic* quantum state described by the macroscopic wavefunction

$$\psi(\mathbf{r},t) = |\psi(\mathbf{r},t)|\, e^{i\phi(\mathbf{r},t)}$$

The phase $\phi(\mathbf{r},t)$ is coherent throughout

0031-9228 / 86 / 0300 36- 09 / $01.00

Biomagnetism. SQUIDs inside the two cryostats shown in this photograph detect magnetic fields emanating from the subject's brain. Each cryostat contains seven second-order gradiometers to detect the signal, and three magnetometers and one first-order gradiometer for electronic cancellation of background noise. The sensors are immersed in liquid helium, which is contained by the superinsulated fiberglass cryostats. (Photograph by Hank Morgan, courtesy of New York University Medical Center and Biomagnetic Technologies Inc.) Figure 1

the superconductor. Thus superconductivity is a macroscopic quantum phenomenon.

The long-range order of the condensate has many important consequences. First, it gives rise to infinite electrical conductivity: A current induced in a superconducting ring is carried by Cooper pairs and persists forever. However, the magnetic flux through the ring generated by this current cannot take arbitrary values but is quantized in units of the flux quantum Φ_0, which is the ratio of Planck's constant to the charge of a Cooper pair: $h/2e$, or about 2×10^{-15} Wb. Thus the enclosed flux Φ is an integral multiple of the flux quantum: $\Phi = n\Phi_0$, $n = 0, 1, 2, \ldots$. This phenomenon of flux quantization[6] is another consequence of the macroscopic wavefunction; the requirement that $\psi(\mathbf{r},t)$ be single valued means that the phase $\phi(\mathbf{r},t)$ must change by exactly $2\pi n$ on going once around the ring.

A third consequence of long-range phase coherence is Josephson tunneling,[6] first proposed by Brian Josephson in 1962. Consider two superconductors separated by a thin, insulating barrier through which Cooper pairs can tunnel quantum mechanically, maintaining phase coherence between the two superconductors in the process. Josephson showed that the difference δ between the phases on the two sides of the junction is related to the supercurrent I flowing through the barrier by the relation $\sin\delta = I/I_0$, where I_0 is the critical current, that is, the maximum supercurrent that the junction can sustain. For applied currents greater than the critical current a voltage V exists across the junction, and the phase difference δ increases with time as $d\delta/dt = 2\pi V/\Phi_0$.

Flux quantization and Josephson tunneling are the essential ingredients of the SQUID.[7,8]

The dc SQUID

Robert Jaklevic, John Lambe, Arnold Silver and James Mercereau were the first to demonstrate[9] quantum interference between two Josephson tunnel junctions connected in parallel as indicated in figure 2a. As they changed the magnetic flux Φ threading the superconducting loop they found that the critical current of the two junctions oscillated with a period equal to the flux quantum Φ_0. These oscillations arise from interference between the macroscopic wavefunctions at the two junctions just as the interference between two coherent light beams in an optical experiment gives rise to bright and dark fringes. This phenomenon of "superconducting quantum interference" forms the basis of a whole technology.

In the conventional mode of dc-SQUID operation, its current–voltage characteristic must be non-hysteretic. One can ensure this by adding an external shunt with a sufficiently low resistance. When the flux through the SQUID is changed, the I–V characteristic oscillates smoothly between two ex-

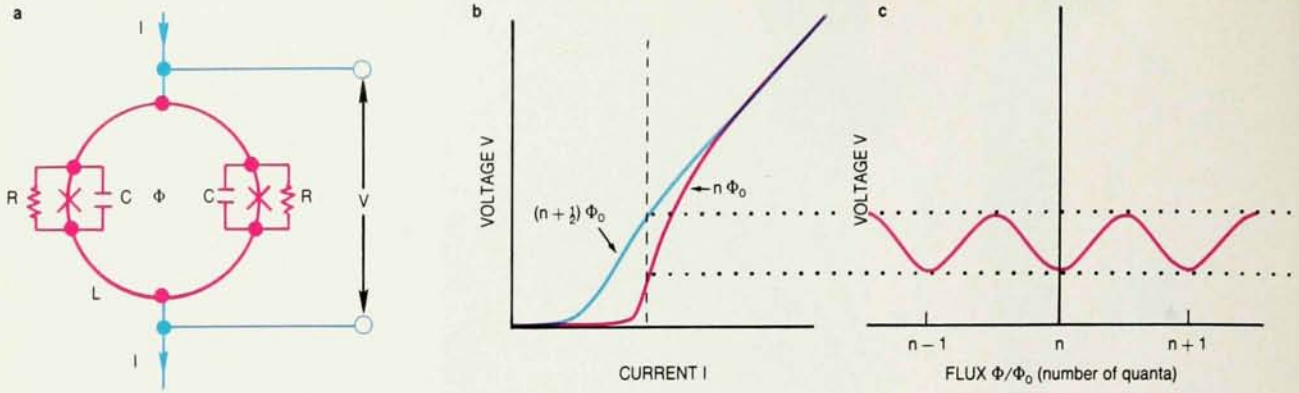

Schematic and electrical characteristics of dc SQUID. The schematic in **a** is that of a dc SQUID biased with a current *I* and a flux Φ. Each of the two Josephson tunnel junctions (indicated by crosses) is shunted with its self-capacitance *C* and an external resistance *R*. The inductance of the loop is *L*. The current–voltage characteristics in **b** are those of a SQUID with fluxes $n\Phi_0$ and $(n + \frac{1}{2})\Phi_0$. The plot in **c** shows the voltage *V* across the SQUID as a function of the flux Φ/Φ_0 at the fixed current bias indicated by the dashed line in **b**.
Figure 2

trema, which are indicated in figure 2b. Thus when the SQUID is biased with a constant current, the voltage across the SQUID is periodic in the applied flux, as shown in figure 2c. One normally operates the device with a flux bias of about $(2n + 1)\,\Phi_0/4$, for which the voltage is almost linear in the applied flux.

Thus, one may usefully think of the SQUID as a flux-to-voltage transducer that converts a change in magnetic flux to a change in voltage readily detectable with conventional electronics. However, because one often needs a dynamic range of flux considerably greater than a fraction of a flux quantum, one usually operates the SQUID as the null detector in a feedback circuit. In this mode any change in voltage across the SQUID produced by an applied magnetic flux is amplified and converted into a current through a coil coupled to the SQUID to produce an equal and opposite flux. (To avoid drifts and low-frequency noise in the electronics, in practice one applies an alternating flux to the SQUID and amplifies the resulting alternating voltage across the device.) In this way, one can not only detect a change in flux of much less than the flux quantum Φ_0 but also measure an applied flux corresponding to many flux quanta. The frequency response of a flux-locked SQUID typically ranges from zero to tens of kilohertz.

What limits the resolution of a dc SQUID? The concept of "flux-noise energy" is useful in addressing this question. If the smallest flux change a SQUID can resolve in a unit bandwidth at a frequency *f* is $\delta\Phi(f)$, one can define a flux-noise energy per unit bandwidth given by $\epsilon(f) = (\delta\Phi)^2/2L$, where *L* is the inductance of the SQUID. The smaller the value of the flux-noise energy $\epsilon(f)$, the better the resolution. The equivalent flux noise $\delta\Phi$ is just the ratio of the voltage noise δV across the SQUID per unit bandwidth to the flux-to-voltage transfer function $\partial V/\partial\Phi$.

To calculate the voltage noise and the transfer function Claudia Tesche and I solved numerically the equations for a SQUID, assuming that the only sources of noise were the two independent Nyquist, or thermal, noise currents produced by the shunt resistors.[7] From this analysis we concluded that with appropriate current and flux biases, the SQUID achieves its optimum noise energy when $2LI_0 \approx \Phi_0$. The optimum noise energy is then

$$\epsilon \approx 10\, k_B T (LC)^{1/2}$$

Here k_B is Boltzmann's constant, *C* is the capacitance of one of the tunnel junctions and *T* is the absolute temperature. The message of this equation is clear: Smaller is better. Thus, if one can decrease the inductance of the SQUID loop or the area and hence the capacitance of the junctions, the noise energy will be correspondingly reduced. Cooling the device to a lower temperature should give further improvement.

Our prediction for the noise energy motivated numerous groups to fabricate a wide variety of devices using thin-film technology pioneered[10] by IBM, Yorktown Heights, for its now downscaled Josephson-computer project. Photolithography or electron-beam lithography can produce tunnel junctions with areas that range from perhaps 5 square microns down to 0.1 square microns or even smaller. The tunnel barriers are grown in a controlled way, usually by oxidation under exposure to an oxygen plasma or ion beam. In this short article I cannot describe all of the devices that have been made and tested. Suffice it to say that the above equation predicts fairly well the dependence of the noise energy on the inductance *L* and capacitance *C*. In a period of a few years the optimum noise energy ϵ has been decreased by about four orders of magnitude. Dale van Harlingen, Roger Koch and I at Berkeley have reported the smallest value of the noise energy ϵ to date, about $2\hbar$, which is only about a factor of 2 higher than the value predicted to be set by zero-point fluctuations in the resistors.[7] Recent work by Frederick Wellstood, Cristian Urbina and myself shows that the temperature dependence predicted by the above equation is valid at least down to 90 mK.

However, one needs not only a sensitive SQUID but also a way of coupling flux into it. Mark Ketchen and Jeffrey Jaycox at IBM took a major step forward in coupling by fabricating a planar device with a thin-film spiral input coil that is overlaid on but electrically isolated from the body of the SQUID. Figure 3 shows a version of this design that is currently the "workhorse" at Berkeley. The body of the SQUID provides a superconducting ground plane to the coil, not only greatly reducing its self-inductance but also forcing most of the magnetic flux generated by a current in the input coil through the SQUID loop. In a flux-locked loop at 4.2 K the flux-noise amplitude is typically $3\times10^{-6}\,\Phi_0$ $\mathrm{Hz}^{-1/2}$, corresponding to a noise energy of a few hundred $\hbar$. Investigators at the National Bureau of Standards in Boulder, Colorado, have successfully fabricated devices based on alternative coupling schemes, one device in-

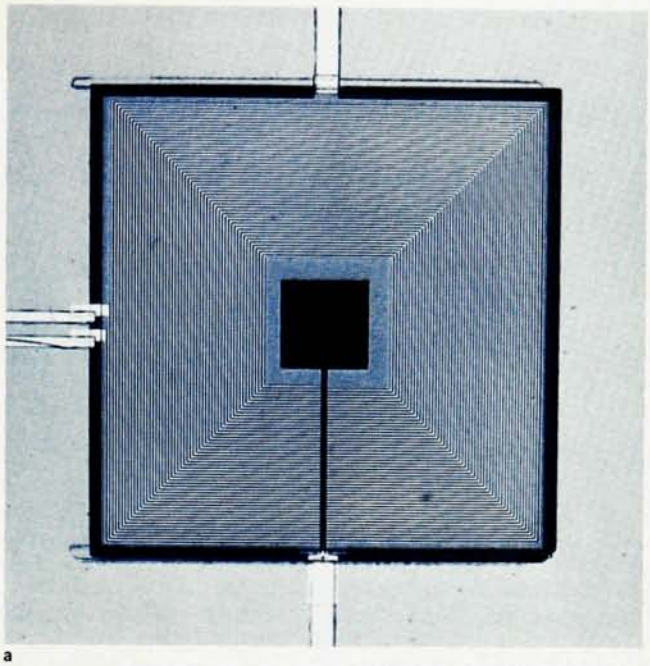

a

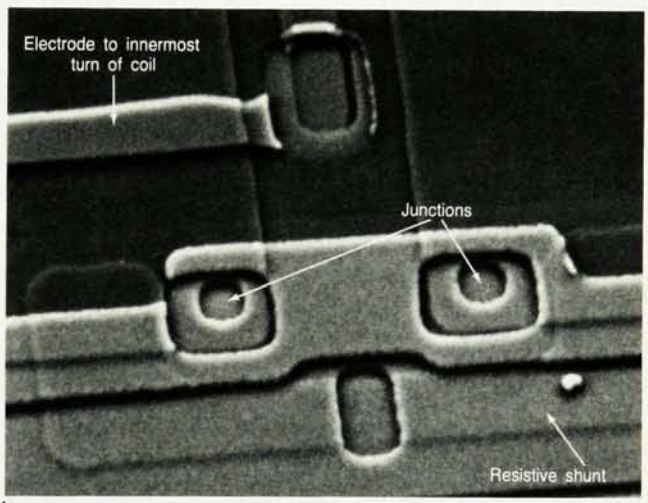

b

SQUID and its Josephson junctions. The planar thin-film dc SQUID whose photograph appears in **a** consists of a square niobium washer (pale blue) with two Josephson junctions at the lower edge, one on each side of the vertical slit. The square washer is 0.9 mm on a side. Each light vertical strip at the top and bottom of the device is a current and voltage lead. The two horizontal leads at the left are the input terminals to the 50-turn coil that overlays the niobium washer. The scanning electron micrograph in **b** shows the Josephson junctions, each of which is about 2.5 microns across. (Photographs courtesy of John Jacobsen, Richard Hall, Claude Hilbert and Frederick Wellstood, University of California, Berkeley, and Lawrence Berkeley Laboratory.) Figure 3

volving a double transformer and another a multi-loop, fractional-turn SQUID.[8]

Like all electronic devices, SQUIDs exhibit "$1/f$ noise," that is, noise with a spectral density that scales inversely with frequency. The origin of this noise, which limits the resolution at low frequencies, is only now becoming understood. The critical current of a single Josephson tunnel junction exhibits $1/f$ noise that arises from the trapping and detrapping of electrons in the barrier,[11] but this effect is too small to account for the $1/f$ noise observed in many SQUIDs. Thus it appears that there is an additional source of $1/f$ noise—conceivably the motion of magnetic flux trapped in the body of the SQUID. SQUIDs fabricated recently at IBM[12] and at Berkeley have shown very low levels of $1/f$ noise, although the physical difference between these and other, much noisier devices is still being investigated.

I should emphasize that although I have focused on the dc SQUID in this article, the rf SQUID[5] is much more widely used, for the simple reason that it has been commercially available since the early 1970s. The rf SQUID consists of a superconducting loop interrupted by a single Josephson junction. The loop is coupled to the inductor of an LC-resonant circuit excited by a radiofrequency current at about 30 MHz. The amplitude of the alternating voltage across the resonant circuit is periodic in the flux threading the SQUID with a period Φ_0, so that with suitable electronics one can operate the rf SQUID in a flux-locked loop in much the same way as one does the dc SQUID. Although the sensitivity of the rf SQUID is not nearly as good as that of the dc SQUID, it is nonetheless adequate for a wide variety of experiments.

SQUID instrumentation

Both dc and rf SQUIDs are almost always used in conjunction with some kind of input circuit, and I will give two brief examples.

One important application of SQUIDs is to the measurement of magnetic field gradients. The flux transformer illustrated in figure 4a can detect the first derivative of the field. Two loops of superconducting wire, wound in opposition and carefully matched, are connected in series with the input coil of a SQUID that is enclosed in a superconducting shield. Application of a uniform axial magnetic field H_z induces no supercurrent because the flux linked by one loop is exactly canceled by the flux linked by the other. On the other hand, application of a magnetic field gradient $\partial H_z/\partial z$ induces a supercurrent in the input circuit to satisfy flux quantization. This current generates a flux in the SQUID, which produces a signal proportional to the gradient.

The loop scheme shown in figure 4b is that of a second-order gradiometer, sensitive to $\partial^2 H_z/\partial z^2$. Gradiometers of the kind shown in figures 4a and 4b, consisting of niobium wire wound on precision-ground quartz cylinders and balanced by adjustable superconducting disks, have been available commercially for more than a decade. One sometimes achieves the final balance in these gradiometers electronically using three orthogonal SQUIDs to measure variations in the magnetic field. One subtracts appropriate components of the SQUID outputs from the gradiometer output to remove the effects of uniform fields, which are characteristic of distant background sources.

Much research is now under way on integrated, thin-film gradiometers

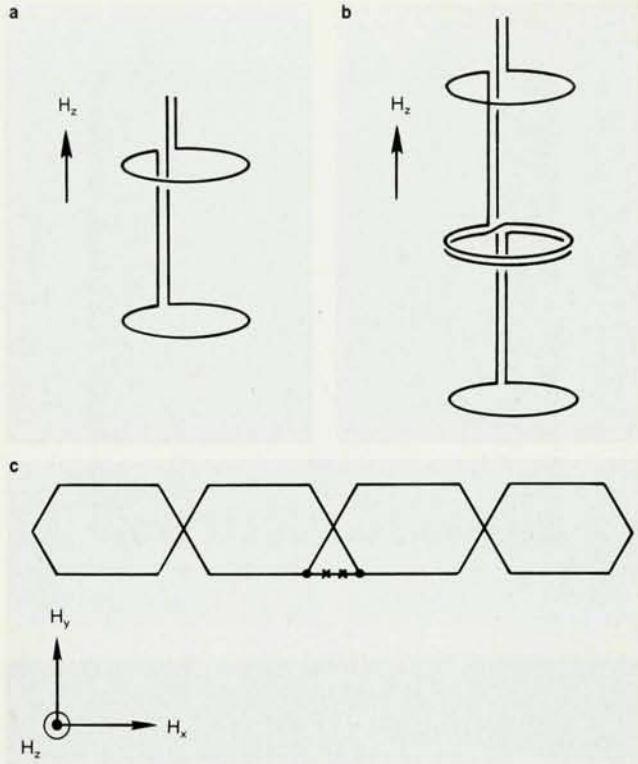

Configurations of gradiometers. The gradiometers in **a** and **b** are made from superconducting wire. The coil geometry in **a** is designed to measure the first-order gradient $\partial H_z/\partial z$. The loops in **b** are sensitive to the second-order gradient $\partial^2 H_z/\partial z^2$. Each gradiometer is connected to the input coil of a SQUID. The configuration in **c** is that of a planar, thin-film, off-diagonal gradiometer that measures $\partial^2 H_z/\partial x^2$. Crossing lines are insulated from each other except at the dots. In the actual device, which is fabricated from niobium films, eight identical gradiometers are connected in parallel with the two junctions that are indicated here by crosses. (Adapted from reference 13.) Figure 4

based on dc SQUIDs. The goal of this work is to develop compact devices that have a high degree of intrinsic balance and therefore require only electronic balancing. The thin-film devices, unlike their wire-wound counterparts, measure off-diagonal gradients such as $\partial^2 H_z/\partial x^2$. Figure 4c shows an example of an off-diagonal gradiometer.[13]

A simple adaptation of the gradiometer enables one to measure magnetic susceptibility. In a commercially available version, one applies a uniform magnetic field along the axis of a first-derivative gradiometer and moves the sample back and forth between the two pickup coils. The resulting peak-to-peak signal from the SQUID is proportional to the magnetization of the sample.

One of the earliest applications of SQUIDs was to the measurement of tiny voltages. This is straightforward at low frequencies: One simply connects the voltage source in series with a cold resistor and the input coil of a SQUID. This routinely gives sensitivities limited by the Nyquist noise in the resistor. For example, one can get a sensitivity of about 10^{-15} V/Hz$^{1/2}$ for a resistance of 10^{-8} Ω. Recently, Claude Hilbert and I developed a dc SQUID for use as a radiofrequency amplifier capable of operating at frequencies up to 100 MHz or higher. In one version we tuned the input circuit by means of a capacitor in series with the input coil. At 93 MHz we achieved a gain of about 18 dB and a noise temperature T_N of about 2 K. (The noise temperature of an amplifier is the temperature to which an input resistor would have to be raised to make the resistor's Nyquist noise, after amplification, equal to the noise of the amplifier.)

The ultimate sensitivity of a SQUID is most conveniently expressed when ones views it as an amplifier. In optimizing a SQUID amplifier one needs to take into account not only the voltage noise across the SQUID but also the current noise circulating in the SQUID loop, which induces a noise in the SQUID amplifier's input circuit. Because there are two noise sources, one cannot completely specify the sensitivity of a SQUID in terms of the flux-noise energy, which does not take into account the current noise. However, one can use instead the noise temperature T_N to characterize a SQUID's performance. For an amplifier tuned to a signal frequency f with a reasonably high quality factor Q, theory indicates[7] that the lowest noise temperature achievable is that of a quantum-limited amplifier, which has a noise temperature T_N of $hf/k_B \ln 2$.

The SQUIDs used in most practical applications operate immersed in liquid helium-4 at a temperature of 1.0–4.2 K. These systems sometimes avoid the use of liquid nitrogen by using specially designed fiberglass cryostats that depend on many layers of superinsulation—aluminized Mylar—to reduce radiation losses to an acceptable level (figure 1). Such cryostats enable one to operate devices for weeks or even months without replenishing the liquid helium.

To avoid relying on liquid helium, however, workers are developing cryocoolers capable of continuous operation at temperatures of a few kelvins. One example is a Sterling-cycle refrigerator built at the National Bureau of Standards by James Zimmerman and operated at temperatures down to about 7 K; another cryocooler, developed at Stanford University by William Little and his coworkers, consists of microchannels etched in thin glass sheets and cools by Joule–Thomson expansion.[14] To make cooling easier, researchers have developed[8] SQUIDs made from materials with superconducting transition temperatures as high as 12 K. The convenience offered by cryocoolers could greatly expand the range of application of SQUIDs and other superconducting devices.

Applications of SQUIDS

Scientists in many fields have put both rf and dc SQUIDs to a remarkably wide range of uses. Laboratory-based measurements performed with SQUIDs include determination of the magnetic susceptibilities of tiny samples over a wide range of temperature, measurement of quasiparticle charge imbalance in superconductors, detection of nuclear magnetic and quadrupole resonance, and noise thermometry, which is the use of noise measurements to determine temperature.

However, SQUIDs long ago left the cryogenics laboratory to serve in applications in which the signal sources are not cryogenic. One area of growing importance is biomagnetism:[15] Investigators have used SQUIDs to study magnetic fields generated by the heart and brain, to detect eye movements and even to detect magnetic impulses generated by isolated frog nerves, to give just a few examples. Another important area is geophysics[1]—magnetotellurics, rock magnetism and paleomagnetism, for example. SQUIDs also see use in relatively large-scale experiments, including gravity-wave antennas,[16] magnetic-monopole detectors (see PHYSICS TODAY, April 1984, page 17) and an orbiting gyro test of general relativity (see PHYSICS TODAY, May

1984, page 20). To illustrate these applications I have deliberately chosen two "noncryogenic" examples—biomagnetism and gravity-wave antennas.

Biomagnetism

David Cohen, Edgar Edelsack and Zimmerman, working at the Francis Bitter National Magnet Laboratory at MIT, were the first to use a SQUID magnetometer to observe[15] the magnetic signal from a biological source when they measured the magnetocardiogram of a human subject enclosed in a magnetically shielded room. In the ensuing 16 years, researchers have studied a wide variety of magnetic signals emanating from living sources. Apart from cardiomagnetism, the major area of research has been neuromagnetism, that is, magnetic fields generated by the neurons in the human brain.

Biomagnetic signals are small, ranging from about 100 picoteslas from the heart to as little as 100 femtoteslas from the brain. Although present-day SQUIDs have a noise level substantially lower than these values, the environmental noise tends to be substantially higher. In a typical laboratory, electric motors, elevators, fans and so on may generate magnetic noise as high as 10 nanoteslas/$Hz^{1/2}$ at a frequency of 1 Hz. The need to eliminate this background noise has been the driving force in the development of the gradiometers described earlier.

Most measurements to date have made use of a second-order axial gradiometer. The lowest pickup loop indicated in figure 4b is placed as close as possible to the subject while the others are sufficiently far away for the magnetic field from the subject to be negligible. Thus one effectively measures the magnetic field generated by the subject while greatly attenuating background fluctuations, which generally have a very small second derivative. This method has given magnetic field sensitivities of about 10 $fT/Hz^{1/2}$. An important alternative or supplementary way of reducing background noise is to enclose the subject and sensor in a room shielded with walls that have either high permeability or high electrical conductivity; the latter provides eddy-current shielding.

In illustrating biomagnetic measurements, I will concentrate on neuromagnetism, which is the object of research[15] in a large number of laboratories in both the United States and Europe. Research in this field falls into two broad areas: evoked response, in which one stimulates the subject with, for example, an electrical, auditory or visual signal; and spontaneous activity.

The ability of the evoked-response technique to localize a source is illustrated by the work[17] at New York University by Gian Luca Romani, Samuel Williamson and Lloyd Kaufman on the response within the auditory cortex to pure tones. The NYU group generated four different tones and used a magnetic gradiometer to measure the responses to each at about 40 points over the scalp. For each tone they found that the spatial distribution of the magnetic field response corresponds approximately to that produced by a current dipole, or short element of

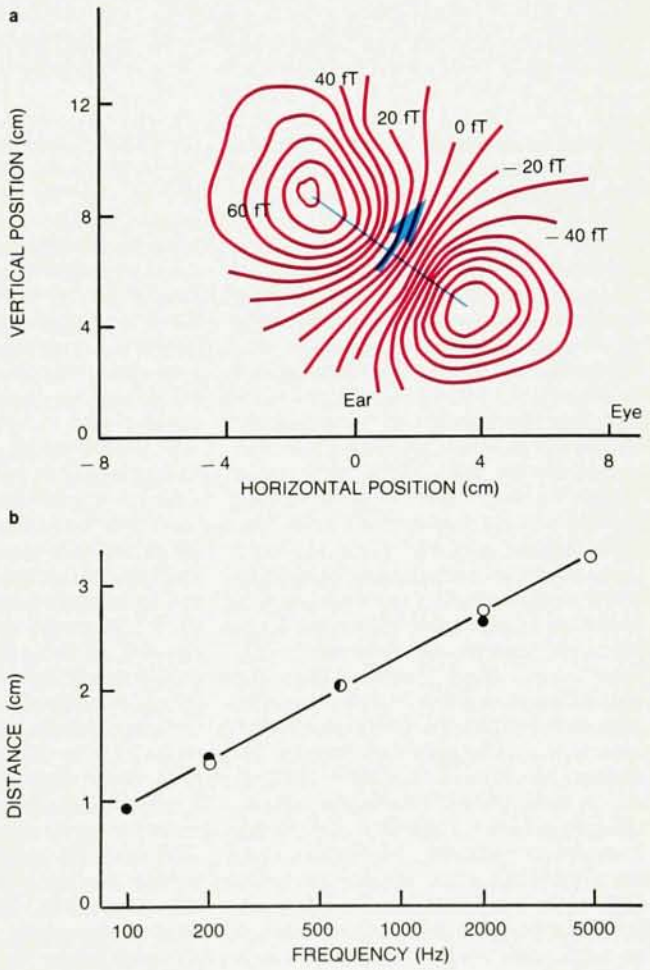

Evoked auditory response. The plot in **a** shows the magnetic field normal to the scalp over the right hemisphere and the position of the equivalent current dipole. The stimulus was a 600-Hz tone. The plot in **b** shows the relative positions of equivalent current dipoles as a function of frequency for two subjects, indicated by open and closed circles. (Adapted from ref. 17.) Figure 5

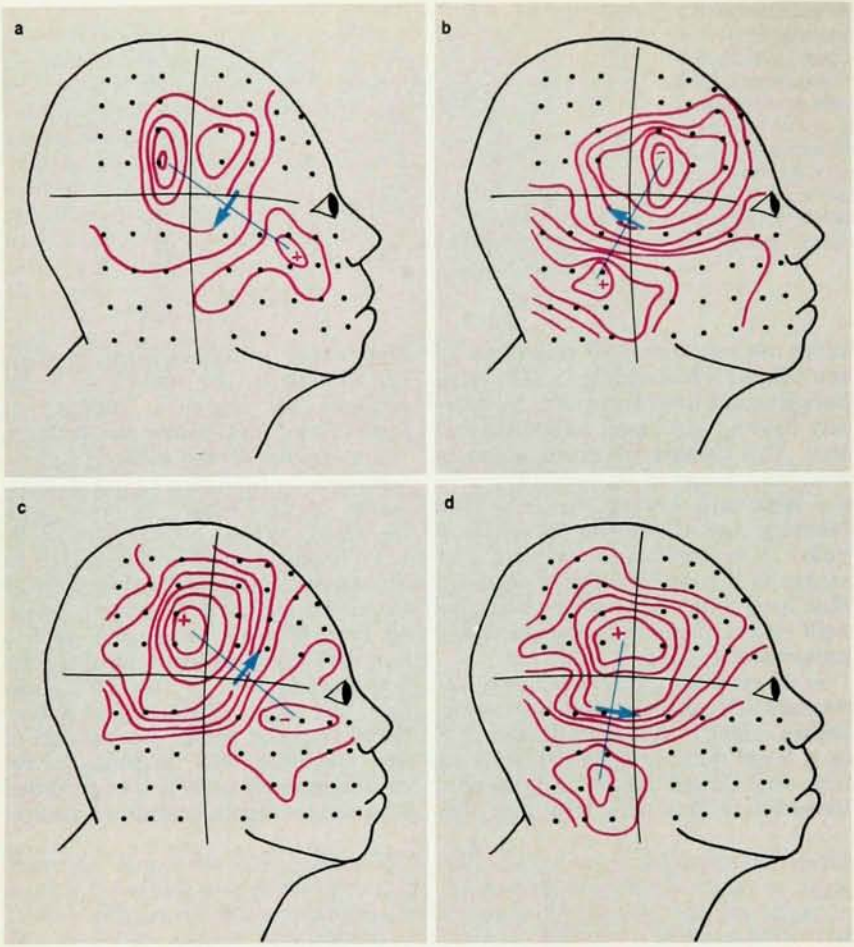

Sequence of magnetic field maps showing the averaged time evolution of an epileptic spike: **a,** initial discharge of source A; **b** (16 msec later), discharge of source B triggered by A; **c, d,** subsequent evolution of sources A and B, respectively. (Adapted from reference 3.) Figure 6

current, beneath the scalp. Figure 5a shows an example. By assuming that the source was a current dipole, Romani and his coworkers were able to deduce the position of the source as a function of frequency. Figure 5b shows the positions of the sources for two subjects, measured from an origin that would correspond to the position of a 20-Hz source. We see that the positions are identical for the two subjects, varying logarithmically with frequency. The location of the point of maximum sensitivity in the cochlea also varies logarithmically with frequency, suggesting a direct mapping of the cochlea onto the auditory cortex.

An important example of spontaneous magnetic activity is focal epilepsy, a disease in which the abnormal brain tissue responsible for seizures is confined to a small region called the epileptic focus. From time to time the neurons within the focus produce a massive, synchronous electrical discharge, resulting in a focal, or restricted, seizure. That the source of the discharge is localized makes surgical removal a possible treatment, but clearly this requires a precise knowledge of its position. Between seizures many patients exhibit single, randomly occurring electric and magnetic spikes.

At the University of California, Los Angeles, Daniel Barth, William Sutherling, Jerome Engel and Jackson Beatty, using a magnetic gradiometer to study 17 subjects with focal epilepsy, demonstrated[3] that it is possible to determine the position of the epileptic focus quite accurately. In 9 of the subjects the spikes appeared to originate from a single source, while in the remainder there appeared to be multiple sources.

The UCLA group measured the normal component of the magnetic field associated with the spikes at approximately 50 locations on each side of the head. At each location they measured the time evolution of at least 20 spikes and averaged the results. Then they produced maps, such as the ones in figure 6, showing the magnetic field at 4-millisecond intervals. The field distribution in figure 6a corresponds to a current dipole in the position indicated, while that in figure 6b, measured 16 msec later, corresponds to a current dipole displaced by approximately 1 cm from the first. These results indicate that the first discharge triggered the second. Parts c and d of the figure show the subsequent development of the dipoles in a and b; note the reversal of the polarities. Both current dipoles were approximately 3 cm below the scalp.

In an attempt to correlate these current dipoles with structural features in the brain, the UCLA group obtained x-ray tomographs at the level indicated by the magnetic gradiometer measurements. They found that both current dipoles lie at the edge of a region of scar tissue, the presence of which could have disturbed nearby neurons sufficiently to induce them to discharge intermittently.

One can emphasize several aspects of these two examples. In at least some cases, one can represent the source of the magnetic field approximately as a current dipole and locate the dipole to within a few millimeters. Furthermore, this type of investigation is entirely *noninvasive*. By contrast, to obtain similar results electrically, one must generally place electrodes on the surface of the brain.

Both examples, however, illustrate a major drawback: They were made with a single gradiometer that had to be moved sequentially to each location, so that data acquisition was exceedingly tedious. A system developed by Biomagnetic Technologies Inc of San Diego has partially alleviated this difficulty. The system consists of seven second-derivative gradiometers coupled to dc SQUIDs; three magnetometers and one first-order gradiometer coupled to rf SQUIDs provide electronic cancellation of background noise. Both types of SQUIDs are machined from niobium in a toroidal configuration, contain junctions made from thin films and are coupled to wire-wound gradiometers or magnetometers. By using two such systems together, as shown in figure 1, one can record data at 14 locations simultaneously, an enormous improvement over taking measurements with a single channel. Nevertheless, one would really like many more channels, and it seems likely that a system with as many as 100 channels will be developed in the next few years; such a system would eliminate the need for sequential measurements. Both wire-wound gradiometers and integrated, thin-film gradiometers appear to offer viable approaches. Producing a 100-channel system will require considerable effort, but the payoff will make it well worthwhile.

Gravitational-wave antenna at Stanford University. (Photograph by Frans Alkemade, courtesy Stanford University.) Figure 7

In addition to the work described here, neuromagnetism has the potential for use in studying other disorders, such as schizophrenia, Parkinson's disease and Alzheimer's disease, as well as in monitoring the effects of treatment of these and other diseases.

Gravity-wave detectors

More than a dozen groups are now involved in a worldwide effort to detect gravitational radiation. The groups are looking specifically for the pulse of gravitational radiation that theory predicts[16] a collapsing star emits. There are two basic types of ground-based antenna: the Weber-bar detector and the laser interferometer. We are concerned here with the first, which consists of a large, freely suspended bar that a passing gravity wave would set into longitudinal oscillation. Because the radiation is exceedingly weak, the anticipated amplitude of the oscillations is small, and many groups are using SQUIDs to detect them.

Figure 7 shows the antenna at Stanford University.[4] The aluminum bar is 3 meters long, weighs 4800 kg and is maintained at a temperature of 4.2 K. The bar's fundamental mode of longitudinal oscillation has a frequency $\omega_a/2\pi$ of 842 Hz with a quality factor Q of 5×10^6. A transducer such as the one sketched in figure 8 detects the longitudinal motion. A circular niobium diaphragm is clamped at its perimeter to one end of the bar, with a flat spiral coil made of niobium wire mounted on each side. The two coils are connected in parallel with each other and with the input coil of a SQUID; this entire circuit is superconducting. A persistent supercurrent circulates in the closed loop formed by the two spiral coils. The associated magnetic fields exert a restoring force on the diaphragm so that, by adjusting the current, one can set the resonant frequency of the diaphragm equal to that of the bar. A longitudinal oscillation of the bar induces an oscillation in the position of the diaphragm relative to the two coils, thereby modulating their inductances. As a result of flux quantization, a fraction of the stored supercurrent is diverted into the input coil of the SQUID, which detects it in the usual way.

The present Stanford antenna has a root-mean-square strain sensitivity $\langle(\delta l)^2\rangle^{1/2}/l$ of 10^{-18}, where l is the length of the bar and δl its longitudinal displacement. This very impressive sensitivity, which is limited by thermal noise in the bar, is nonetheless adequate only to detect events in our own galaxy. Because such events are rare, there is a very strong motivation to make major improvements in the sensitivity.

If the bar could be cooled sufficiently, the strain resolution would be limited only by the bar's zero-point motion and would have a value of about 3×10^{-21}. At first sight one might expect that the bar would have to be cooled to an absurdly low temperature to achieve this quantum limit, because a frequency of 842 Hz corresponds to a temperature $\hbar\omega_a/k_B$ of about 40 nK. However, it turns out that one can make the effective noise temperature T_{eff} of the antenna much lower than the temperature T of the bar. If a gravitational signal in the form of a pulse of length τ_s interacts with an antenna that has a decay time Q/ω_a, then the effective noise temperature is given[18] approximately by the product of the bar temperature and the pulse length divided by the decay time: $T_{eff} \approx \tau_s\omega_a T/Q$. Thus one can make the effective noise temperature much less than the temperature of the bar by increasing the bar's resonant quality factor sufficiently. To achieve the quantum limit, in which the bar energy $\hbar\omega_a$ is greater than the effective thermal energy $k_B T_{eff}$, one would have to lower the temperature T below $Q\hbar/k_B\tau_s$, which is about 40 mK for a quality factor Q of 5×10^6 and a pulse length τ_s of 1 msec. One can reasonably expect that it will be possible to cool the antenna to this temperature with the aid of a large dilution refrigerator.

Needless to say, to detect the motion of a quantum-limited antenna requires a quantum-limited transducer. This requirement has been a major driving force in the development of ultra-low-noise dc SQUIDs. Existing SQUID amplifiers that can couple effectively to inductances of about 1 μH are roughly two orders of magnitude from the quantum limit when operating in the temperature range of liquid helium-4. Thus, according to the noise-energy equation on page 38, if one were to cool such a device to, say, 40 mK and shrink its dimensions by a modest amount, one might hope to achieve the quantum limit. There are two provisos: Joule heating must not raise the temperature of the resistive shunts significantly above the bath temperature, and $1/f$ noise must be negligible at the 1-kHz resonant frequency of the bar. Preliminary experiments at Berkeley indicate that the first problem is not a serious one but that the second may be. Nonetheless, there is reason to believe that an amplifier with a noise temperature near the quantum limit at 1 kHz will be available in the near future.

Of course many other problems stand in the way of a quantum-limited antenna, not the least of which is external and internal parasitic vibrational noise. Furthermore, a bar with a mass of about 5000 kg operated at the quantum limit will have sufficient sensitivity to detect only the strongest predicted events in nearby galaxies; these events are expected to occur at a rate of perhaps one per year. To achieve higher sensitivity with a linear transducer and amplifier, and thereby

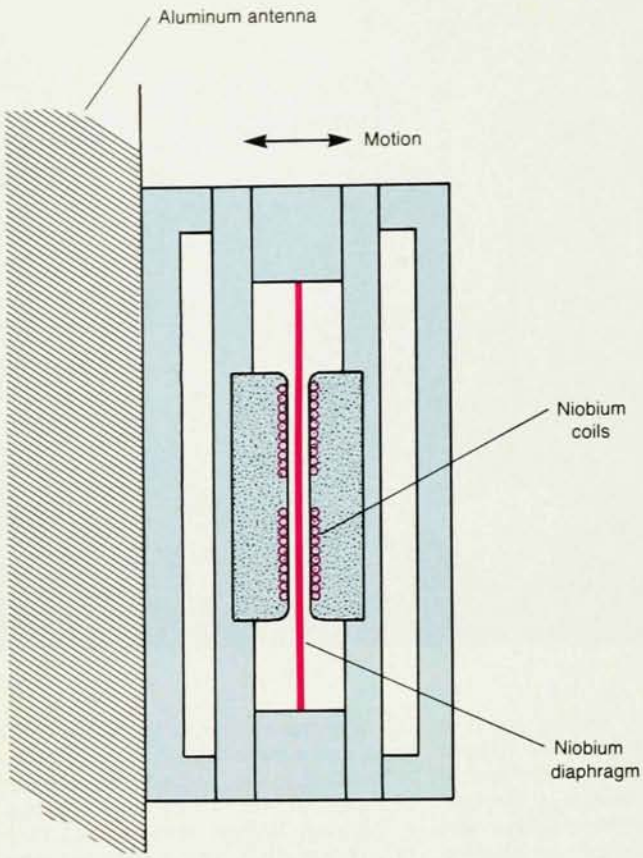

Motion transducer for gravity-wave antenna. The entire transducer is about 6.5 cm thick. (Adapted from reference 4.) Figure 8

increase the rate of detection of events, one must increase the mass of the bar. The best way to do this is to build a number of detectors that can operate in coincidence and thereby discriminate against local noise sources. Another possibility is to increase the sensitivity of a single antenna beyond the quantum limit by "quantum nondemolition,"[19] a proposed technique in which one would get a very precise measurement of the real part of the complex amplitude of the motion while forgoing all knowledge of the imaginary part. This technique would in principle enable one to measure an arbitrarily weak classical signal with arbitrary accuracy.

• • •

Part of the research that I have described in this article was carried out at Berkeley over the last 12 years, and I wish to thank my coworkers Wolf Goubau, Gil Hawkins, Claude Hilbert, Mark Ketchen, Roger Koch, John Martinis, Claudia Tesche, Cristian Urbina, Dale van Harlingen and Fred Wellstood for their dedicated and enthusiastic efforts. I have also enjoyed fruitful collaborations with Gordon Donaldson, Robin Giffard, Bob Laibowitz, Colin Pegrum, Stan Raider and Dick Voss. Samuel Williamson and Peter Michelson kindly provided much useful information on biomagnetism and gravitational-wave detectors, respectively, and supplied figures 1 and 7. I am grateful to Allan Mackintosh for a critical review of the manuscript, and to the members of Physics Laboratory I of the H. C. Ørsted Institute, University of Copenhagen, for their hospitality during its preparation. Those portions of the work carried out at Berkeley were supported by the Office of Basic Energy Sciences, Materials Sciences Division, US Department of Energy, under contract number W-7405-ENG-48.

References

1. For a review of geophysical applications, see J. Clarke, IEEE Trans. Magn. **MAG-19**, 288 (1983).
2. T. Sleator, E. L. Hahn, C. Hilbert, J. Clarke, Phys. Rev. Lett. **55,** 1742 (1985)
3. D. S. Barth, W. Sutherling, J. Engel Jr, J. Beatty, Science **223,** 293 (1984).
4. M. Bassan, W. M. Fairbank, E. Mapoles, M. S. McAshan, P. F. Michelson, B. Moskowitz, K. Ralls, R. C. Taber, in *Proc. 3rd Marcel Grossmann Meeting on General Relativity*, H. Ning, ed., North Holland, New York (1983), p. 667.
5. J. E. Zimmerman, P. Thiene, J. T. Harding, J. Appl. Phys. **41,** 1572 (1970).
6. See, for example, M. Tinkham, *Introduction to Superconductivity*, McGraw–Hill, New York (1975).
7. For a detailed description of SQUIDs and copious references, see: J. Clarke, in *Superconductor Applications: SQUIDs and Machines*, B. B. Schwartz, S. Foner, eds., Plenum, New York (1977), p. 67; J. Clarke, IEEE Trans. Electron Devices **ED-27,** 1896 (1980); J. Clarke, in *Advances in Superconductivity*, B. Deaver, J. Ruvalds, eds., Plenum, New York (1983), p. 13.
8. For collections of papers on SQUIDs, see the proceedings of the applied-superconductivity conferences. The last three proceedings are in IEEE Trans. Magn. **MAG-17,** no. 1 (1981); **MAG-19,** no. 3 (1983); **MAG-21,** no. 2 (1985). Also see the *Proc. Int. Conf. on Superconducting Quantum Interference Devices and Their Applications*, H. D. Hahlbohm, H. Lübbig, eds., Walter de Gruyter, Berlin (1977), (1980), (1985).
9. J. C. Jaklevic, J. Lambe, A. H. Silver, J. E. Mercereau, Phys. Rev. Lett. **12,** 159 (1964).
10. See IBM J. Res. Dev. **24,** no. 2 (March 1980).
11. C. T. Rogers, R. A. Buhrman, Phys. Rev. Lett. **53,** 1272 (1984); R. H. Koch, in *Noise in Physical Systems*, M. Savelli, G. Leroy, J. P. Nougier, eds., North Holland, New York (1983), p. 377.
12. C. D. Tesche, K. H. Brown, A. C. Callegari, M. M. Chen, J. H. Greiner, H. C. Jones, M. B. Ketchen, K. K. Kim, A. W. Kleinsasser, H. A. Notarys, G. Proto, R.H. Wang, T. Yogi, *Proc. 17th Int. Conf. on Low Temperature Physics*, U. Eckern, A. Schmid, W. Weber, H. Wuhl, eds., North Holland, New York (1984), p. 263.
13. G. J. van Nieuwenhuyzen, V. J. de Waal, Appl. Phys. Lett. **46,** 439 (1985).
14. J. E. Zimmerman, in *Superconducting Quantum Interference Devices and Their Applications*, H. D. Hahlbohm, H. Lübbig, eds., Walter de Gruyter, Berlin (1980), p. 423; W. A. Little, Rev. Sci. Instrum. **55,** 661 (1984).
15. For extensive reviews, see S. J. Williamson, L. Kaufman, J. Magn. Magn. Mater. **22,** 129 (1981); S. J. Williamson, G. L. Romani, L. Kaufman, I. Modena, eds., *Biomagnetism: An Interdisciplinary Approach*, Plenum, New York (1983).
16. For an elementary review on gravity waves, see S. L. Shapiro, R. F. Stark, S. J. Teukolsky, Am. Sci. **73,** 248 (1985).
17. G. L. Romani, S. J. Williamson, L. Kaufman, Science **216,** 1339 (1982).
18. R. P. Giffard, Phys. Rev. A **14,** 2478 (1976).
19. For a review, see C. M. Caves, K. S. Thorne, R. W. P. Drever, V. D. Sandberg, M. Zimmermann, Rev. Mod. Phys. **52,** 341 (1980). □